ARIES-Note 2018-001

A High-Brilliance Angstrom-FEL based on the LHeC

Z. Nergiz
*Nigde Omer Halisdemir University, Faculty of Arts and Sciences, Physics Department, 51200 Nigde, Turkey**

F. Zimmermann
CERN, 1211 Geneva 23, Switzerland

H. Aksakal
Kahraman Maras Sutcu Imam University, 46040 Kahramanmaras, Turkey
(Dated: July 18, 2018)

The Large Hadron electron Collider (LHeC) is a proposed future particle physics project colliding 60 GeV electrons from a recirculating energy-recovery linac (ERL) with 7 TeV protons stored in the LHC. The ERL technology allows for much higher beam current and, therefore, higher luminosity than a traditional linac. The high-current high-energy electron beam can also be used to drive a free electron laser (FEL). In this study we investigate the performance of an LHeC based FEL, operated in the self-amplified spontaneous emission mode, for which we choose a final electron beam energy of 40 GeV and aim for X-ray wavelengths of less than 1 Å. We demonstrate that such FEL would have the potential to provide orders of magnitude higher peak power, peak brilliance and average brilliance, than any other FEL either existing or proposed.

PACS numbers: Valid PACS appear here

I. INTRODUCTION

One of the most important parameters of a collider is its luminosity. To achieve a high luminosity the beam current should be as high as possible and the transverse sizes of the particle beams at the collision point should be as small as possible. In the case of the proposed lepton-hadron collider based on the LHC (LHeC), unusually, the impact of the electron beam size on the luminosity is rather limited, since the proton beam size is large by electron-beam standards and cannot easily be reduced. Therefore, the electron beam current should be made as high as possible to achieve a high luminosity. To increase the electron beam current for a linac-based collider the energy recovery linac option is a cost-efficient choice, which has been adopted for the LHeC baseline design [1].

The high current ERL of the LHeC would also provide the opportunity for driving a Free Electron Laser (FEL) [2]. Indeed ERL-based FELs already operated, and operte, successfully in the electron energy range of 10 to 200 MeV, e.g. at BINP[3], JAEA [4] and JLAB [5], whose parameters are compiled in Table I. A superconducting energy recovery linac with a higher beam energy of 0.5–1.0 GeV was proposed to produce 13.5 nm radiation, at 5 kW average power [6]. Most similar to the LHeC-FEL, however, would be a possible upgrade of the European XFEL, based on an ERL-type of operation, with 100% duty factor and an average brightness brightness of 1.64×10^{25} photons/s/mm^2/mrad^2/0.1% bandwidth at 8.5 GeV beam energy [7].

Though the LHeC is designed for energy frontier electron-hadron scattering experiments at the LHC, it is conceivable that the ERL programme can be temporarily redefined,independently of elepton-hadron operation, as, for example, during the decade in which the LHC may possibly be reconfigured to double its hadron beam energy, and during which no lepton-hadron collisions would take place.

TABLE I: Parameters of some operating ERL-based FELs at lower beam energy.

facility	BINP[3]	JAEA[4]	JLAB[5]
beam energy [MeV]	20	17	120
peak current [A]	3000	35	300
average current [mA]	100	8	8
photon wavelength [μm]	40	22	1.6
average FEL power [W]	500	1	10,000
pulse duration [ps]	50	0.32	0.17

II. ADAPTING THE LHeC BEAM

The ERL of LHeC is of racetrack shape. A 500-MeV electron bunch coming from the injector is accelerated in each of the two 10-GeV SC linacs during three revolutions, after which it has obtained an energy of 60 GeV. Three additional revolutions, now with deceleration instead of acceleration, reconvert the energy stored in the beam back to RF energy [1]. The beam emittance and the energy spread of the particle beam increase with beam energy due to quantum fluctuations.

For the LHeC proper, the electron beam emittance is not critical, since the proton beam emittance is quite large. On the contrary, in order to reach low wavelengths in FEL operation the beam emittance must be

*Electronic address: znergiz@ohu.edu.tr

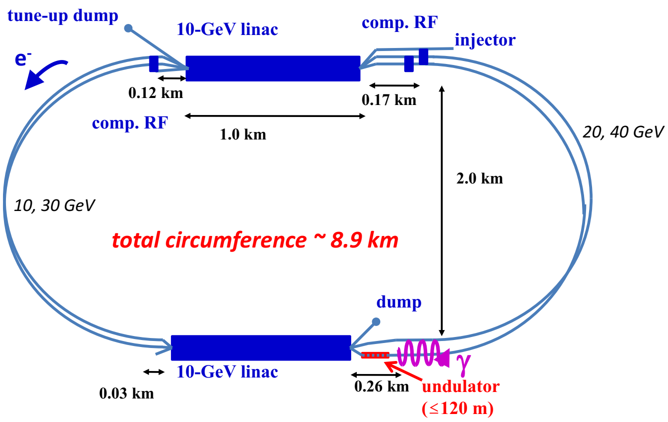

FIG. 1: LHeC recirculating linac reconfigured for FEL operation.

sufficiently small. Because of this requirement, we choose the electron beam energy for FEL operation as 40 GeV, rather than 60 GeV. At a beam energy of 40 GeV, the accumulated relative energy spread induced by quantum fluctuations is 5×10^{-5} and the accumulated normalized emittance due to synchrotron radiation in the LHeC arcs is 0.5 μm [1]. If necessary or useful, the latter number could be reduced by various optics modifications, e.g., by shortening the length of the arc cells. The beam energy of 40 GeV can be attained after two passes through the two 10 GeV linacs, instead of the 3 passes of the standard LHeC operation. The subsequent deceleration would also happen during 2 additional passes. Figure 1 illustrates the LHeC-FEL configuration.

Table II presents the electron beam parameters which we have chosen for our LHeC-FEL study. We assume that the bunch can be compressed to an rms length of 7 μm at the location of the undulator. For comparison, at LCLS-II the rms bunch length can be varied between 0.6 and 52 μm, with a nominal value of 8.3 μm [8]. The nominal rms bunch length of the European X-FEl is 25 micron [9].

Compared with a single-pass linac, a recirculating linac offers additional degrees of freedom to compress the bunch and also to taylor its longitudinal profile, respectively, by exploiting the linear momentum compaction in the return arcs and by controlling the second-order momentum compaction through arc sextupole magnets.

III. FEL CONSIDERATIONS

In a free-electron laser, the active medium is a beam of relativistic electrons. The FEL interaction amplifies the undulator radiation in the forward direction, leading to an exponential growth of the radiation power along the length of the undulator. A self-amplified spontaneous emission (SASE) FEL does not require any optical cavity, nor any coherent seed, and it can operate in the X-ray regime. The wavelength of the radiation is given by the

TABLE II: The main LHeC-ERL electron beam parameters.

Parameters	Unit	Value
energy	GeV	40.0
relativistic gamma		78277.9
electrons per bunch		3×10^9
rms bunch length	μm	7
peak beam current	kA	8.2
average beam current	mA	$\sim$20
normalized emittance	μm	0.5
bunch spacing	ns	25
rms energy spread	%	0.1

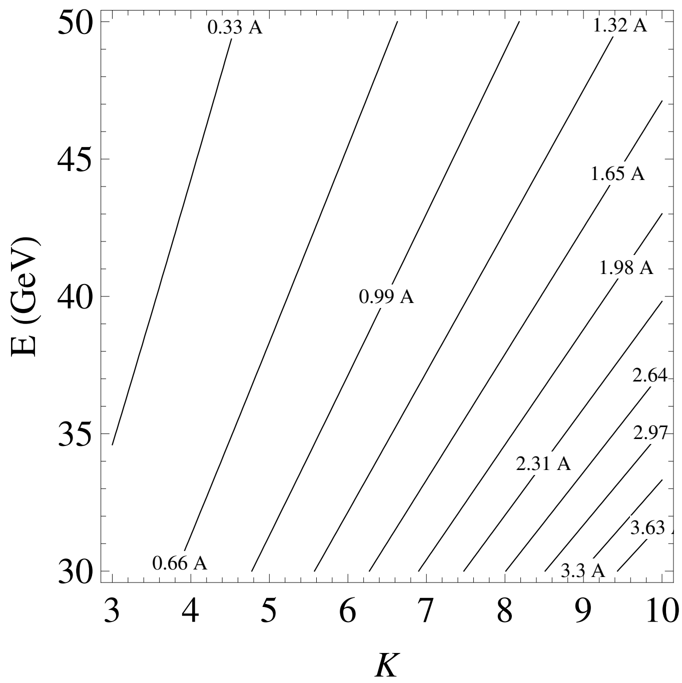

FIG. 2: FEL wavelength (contours) as a function of electron beam energy (vertical axis) and undulator parameter (horizontal axis).

well-known formula

$$\lambda = \frac{\lambda_u}{2\gamma^2}\left(1+\frac{K^2}{2}\right) \qquad (1)$$

where λ_u denotes the period length of a planar undulator, γ the relativistic factor, proportional to the electron energy, and K the undulator parameter [10]. The relation between the radiation wavelength, the electron beam energy and the undulator strength is illustrated in Fig. 2.

The optimum matching of the electron beam to the light beam is achieved under the condition

$$\varepsilon_N \leq \gamma\frac{\lambda}{4\pi} \qquad (2)$$

where $\varepsilon_N \equiv \gamma\varepsilon$ signifies the normalized emittance. However, it has been demonstrated that FELs can still operate, albeit with a reduced efficiency, even if the normalized emittance exceeds this optimum condition by a factor of four to five [11]. Consequently, we expect that FEL light of wavelength around 0.5 Å can be produced by 40 GeV electrons with a normalized rms emittance of 0.5 μm.

IV. UNDULATOR

Harder X-rays with photon energies exceeding 10 keV ($\lambda < 1.2$ Å) are desirable for the study of thick 3D materials due to their deep penetration and excellent spatial resolution. Such X-ray radiation allows probing condensed matter systems on the atomic length scale at minimum unwanted absorption, preserved scattering cross sections and large momentum available [8].

The concrete goal of our LHeC-FEL design is to generate hard X-ray FEL radiation in the range between 0.45 Å and 2.2 Å. We examine the FEL performance of the LHeC-based FEL for an undulator with a period of 55 mm undulator similar to the soft X-ray undulator of LCLS-II.

The relation between the peak magnetic field and undulator parameter is

$$K = 0.934B[\mathrm{T}]\ \lambda_u[\mathrm{cm}] \qquad (3)$$

where K designates the undulator strength parameter, B the peak magnetic field for a planar undulator and λ_u the undulator period. Specifically, to obtain an undulator strength between 4.24 and 9.9, the magnetic field should be between 0.825 and 1.92 T.

Our undulator design, named U55, is of hybrid planar type, made from NdFeB (remanent magnetization B_r=1.25 T) as magnetic material and pure iron as pole material. The magnet model of the U55 is shown in Fig. 3. The undulator period is 55 mm. The dimensions of the magnet material and pole material are chosen as $75 \times 18.5 \times 65$ mm^3 and $50 \times 9 \times 50$ mm^3, respectively. The period of 55 mm corresponds to $2 \times (18.5 + 9)$ mm.

The vertical magnetic field (z coordinate) along the y axis (where y indicates the beam direction) has been computed using the computer code Radia [12]. The peak magnetic field is 1.92 T for 7.2 mm gap, 1.26 T for 12.4 mm and 0.825 T for 17.7 mm gap. The result for a gap of 12.4 mm is presented in Fig. 4.

The undulator parameters are shown in Table III. The targeted wavelengths can be produced by tuning the K values through changing the gap of the undulator.

TABLE III: Main parameters of the LHeC-FEL undulator.

parameter	value
period length (cm)	5.5
number of period	61
total length (m)	120
minimum gap (mm)	7.2
“undulator parameter” K	4.2–9.9
wavelength range (Å)	0.45–2.24

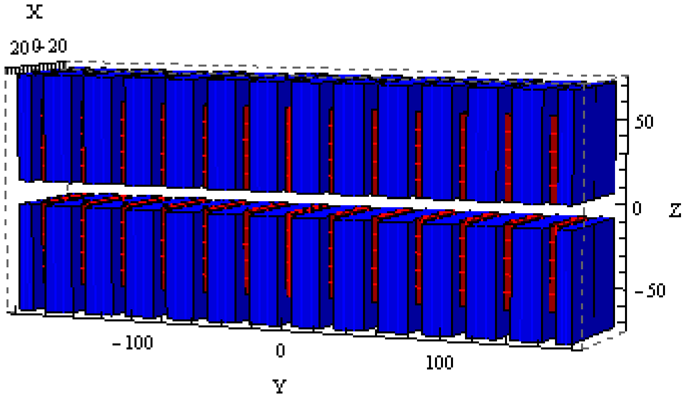

FIG. 3: Magnet arrays of undulator. The permanent magnet elements are shown in blue and the iron poles in red. All the units are in mm. Only the first few periods are shown for clarity.

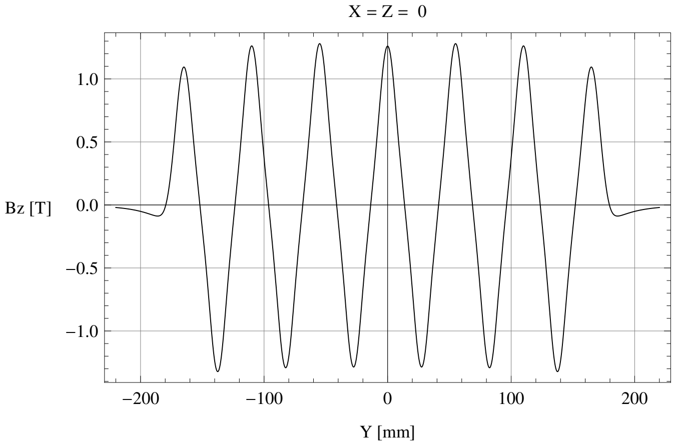

FIG. 4: Vertical magnetic field along the axis of the U55 undulator for a gap of 12.4 mm; only a few periods are shown for clarity.

V. SIMULATED FEL PERFORMANCE

FEL simulations are performed using the GENESIS code [13] for K values of 4.24, 6.5 and 9.9, corresponding to the wavelengths 0.45 Å, 1 Å and 2.24 Å, respectively. A FODO lattice was selected for its simplicity of design and cost-effectiveness through limiting the total number of magnets and associated instrumentation. The length of each undulator is 3.35 m. Undulator modules are separated by intervals of 66 cm, providing some space for focusing, steering, diagnostics or vacuum-system components. Figure 5 shows the simulation results for the case K=4.24. The saturation occurs after a distance of 110 m and the peak power is approximately 120 GW. The results of the simulations for K=6.5 and K=9.9 are shown in Figs. 6 and 7, respectively. For 1 Å laser wavelength the saturation occurs after 85 m, with a peak power of 300 GW, while the saturation occurs already at 70 m with a peak power of 600 GW in case of 2.24 Å FEL wavelength.

One of the important parameters for comparing different radiation sources is the brilliance [14]. It describes the intensity of a light source including its spectral purity and opening angle. The brilliance can be calculated from the spectral flux (in units of photons/s/0.1% bandwidth) by

$$B = \frac{\text{spectral flux}}{4\pi^2 \Sigma_x \Sigma'_x \Sigma_y \Sigma'_y} \ , \tag{4}$$

with the quantities

$$\Sigma = \sqrt{\sigma_e^2 + \sigma_{ph}^2} \tag{5}$$

and

$$\Sigma' = \sqrt{\sigma_e'^2 + \sigma_{ph}'^2} \ . \tag{6}$$

Where σ_e, σ'_e, σ_{ph} and σ'_{ph} are the transverse sizes and angular divergences of electron and photon beams [15]. In the case of full transverse coherence $\Sigma\Sigma' = \lambda_{ph}/(4\pi)$. The brilliance values for the three cases are compiled in Table III, along with some other FEL parameters. A comparison of the LHeC-FEL with a few existing or planned hard X-ray FEL sources is presented in Figs. 8 and 9 [8, 9, 11, 16]. The figure demonstrates that the brilliance of the LHeC-FEL is extremely high. The exceedingly brilliant beam with ultra short (80 fs) pulses at wavelengths below 1 Å could potentially revolutionize scientific experiments in different fields such as physics, biology, chemistry and material science.

Since the LHeC recovery linac provides a high-current high-energy cw electron beam, the average brilliance of the LHeC-FEL is greater by nearly 4 orders of magnitude than for any other FEL source in operation or under construction. It also is three orders of magnitude higher than the projected average brightness predicted for ERL-extensions of presently existing X-ray FEL infrastructures [7].

The high average brilliance of the LHeC-FEL will facilitate the detection of ultrafast changes of structures and the electronic states of natural and artificial materials [17]. To give but one example, studies of nano-materials for advanced battery technologies would greatly profit from the high average brilliance available at the LHeC-FEL [18].

Due to the energy recovery process the energy loss and energy spread of the electron beam after the lasing process are important parameters. The evolution of these parameters for a wavelength of 0.45 Å is shown in Fig. 10. The energy loss at the saturation point is approximately 3.9 MeV. This value is low compared with the electron beam energy, and also with the electron injection energy of 500 MeV, and its effect can easily be accommodated by phasing in the downstream linac. The energy spread increases approximately four times (from 0.1% to 0.4%). The energy spread is small compared with the energy acceptance of the optics, and could also be partially corrected in the downstream arcs and linacs.

TABLE IV: LHeC-FEL radiation parameters derived from simulations. The peak-power values were obtained by averaging the simulated power over the length of the pulse ($\pm\sigma_z$). The unit for the corrresponding peak and average brilliance (B) is equal to photons/mm^2/mrad^2/s/0.1%bw.

parameters	Unit	K=4.24	6.5	9.9
electron energy	GeV	40	40	40
wavelength	nm	0.045	0.1	0.225
photon energy	keV	27.7	12.41	5.54
saturation length	m	110	85	70
peak power	GW	40	65	120
pulse duration	fs	60	60	60
bandwidth	%	0.04	0.05	0.09
photons per pulse	#	5.2×10^{11}	2.5×10^{12}	7.8×10^{12}
peak brilliance	B	4.5×10^{34}	2.6×10^{34}	1.2×10^{34}
average brilliance	B	1.0×10^{29}	6.0×10^{28}	2.8×10^{28}

VI. CONCLUSIONS

We have investigated the potential radiation properties of a SASE FEL based on the LHeC Energy Recovery Linac. As an example, and for the purpose of this study, we considered an LCLS-II type undulator with 55 mm period. Our simulations of the FEL process, for a 40 GeV LHeC electron beam passing through such an undulator, suggest that FEL radiation in the Ångstrom or sub-Ångstrom wavelength regime can be produced, at an exceedingly high peak power and brilliance. Indeed, the LHeC-FEL promises both peak and average brilliance far exceeding those of other, existing or proposed X-ray FELs. For example, at a wavelength of 0.45 Å, saturation occurs around 110 m, with a peak power of 120 GW, and peak brilliance of 4.5×10^{34} photons/mm^2/mrad^2/s/0.1%bw. The beam is cw with a 25 ns bunch spacing, translating into a remarkable average brilliance (see Fig. 9 and Table IV).

The reported simulation results were obtained for the SASE mode of operation and without any tapering. By using self seeding and a tapered undulator the performance could be further improved and the spectrum be rendered more monochromatic.

Acknowledgments

We thank Herwig Schopper, the Chair of the LHeC International Advisory Committee, for suggesting the use of the LHeC as an FEL. We also acknowledge continued encouragement from Oliver Brüning and Max Klein.

This work was supported by the Turkish Atomic Energy Agency with Grant No. 2015 TAEK (CERN) A5.H6.F2-13, and also, in part, by the European Commission under the HORIZON2020 Integrating Activity project ARIES, grant agreement 730871.

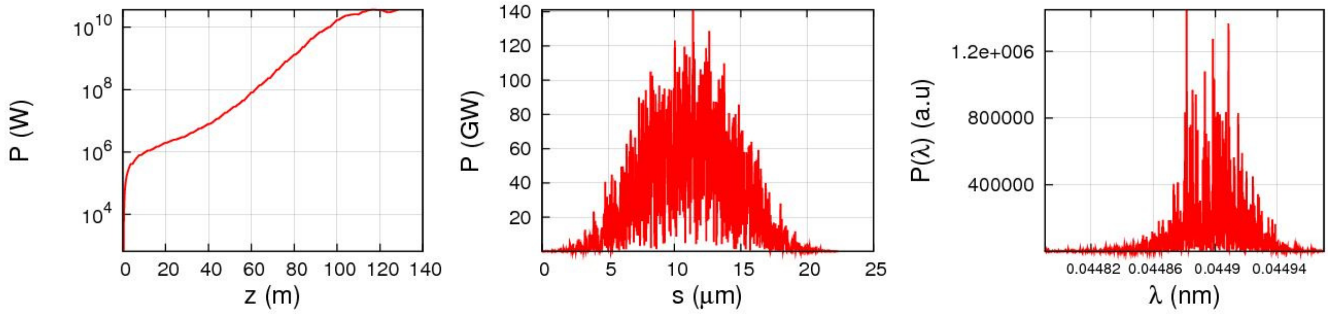

FIG. 5: Genesis simulation results for 0.45 Å laser wavelength ($K = 4.24$). Left: Evolution of the pulse power along the undulator. Middle: Spatial (temporal) profile of the radiation pulse. Right: Wavelength spectrum of the radiation.

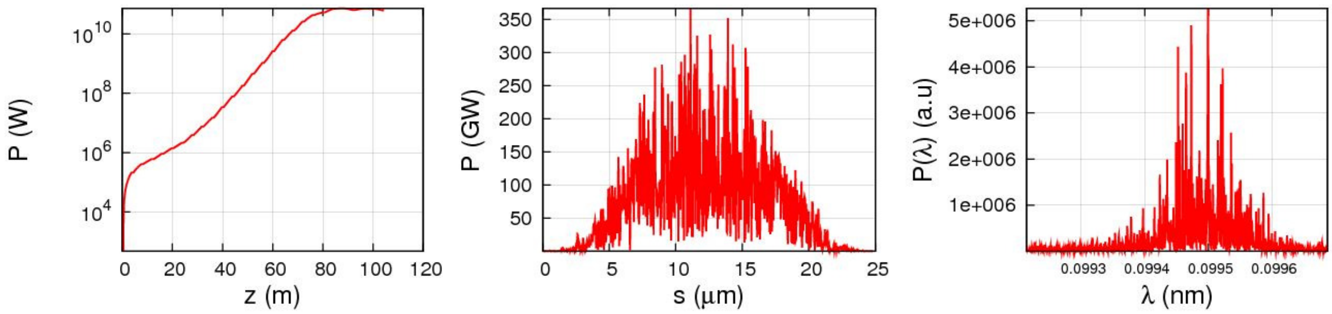

FIG. 6: Genesis simulation results for 1 Å laser wavelength ($K = 6.5$). Left: Evolution of the pulse power along the undulator. Middle: Spatial (temporal) profile of the radiation pulse. Right: Wavelength spectrum of the radiation.

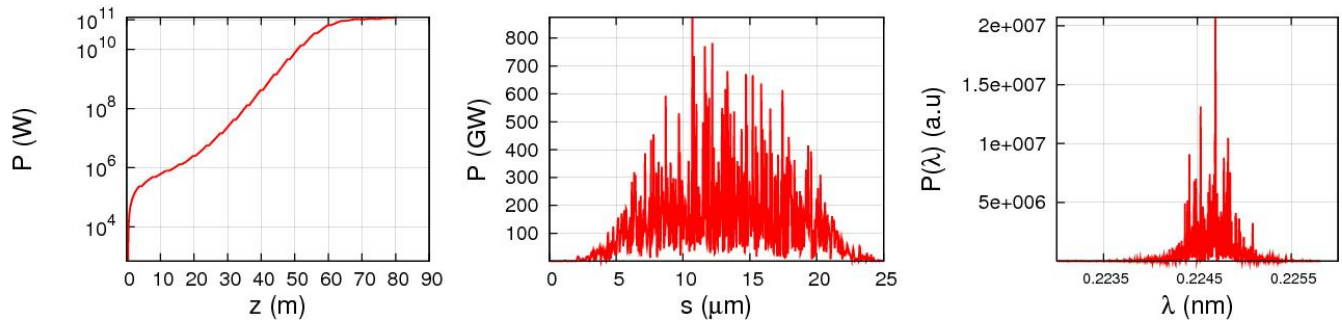

FIG. 7: Genesis simulation results for 2.24 Å laser wavelength ($K = 9.9$). Left: Evolution of the pulse power along the undulator. Middle: Spatial (temporal) profile of the radiation pulse. Right: Wavelength spectrum of the radiation.

[1] J. L. A. Fernandez et al., Journal of physics G: Nuclear and Particle Physics **39**, 075001 (2012).
[2] H. Schopper, suggestion during the 2017 LHeC/FCC-eh workshop (2017), `https://indico.cern.ch/event/639067`.
[3] N. Vinokurov et al., Proc. IPAC'17, Copenhagen p. 4836 (2017).
[4] N. Nishimori and others, Proc. FEL 2006, BESSY, Berlin p. 265 (2006).
[5] S. Benson and others, Proc. PAC07, Albuquerque, New Mexico p. 79 (2007).
[6] Y. Socol, G.N. Kulipanov, A.N. Matveenko, O.A. Shevchenko, and N.A. Vinokurov, Phys. Rev. ST Accel. Beams **14**, 040702 (2011).
[7] J. Sekutowicz et al., Phys. Rev. ST Accel. Beams **8**, 010701 (2005).
[8] Tech. Rep. SLAC-I-060-003-000-02-R003 (2011).
[9] M. Altarelli et al., Tech. Rep. DESY 2006-097 (2006).
[10] H. Wiedemann, *Synchrotron Radiation* (Springer, 2003).
[11] R. Ganter et al., Tech. Rep. PSI Bericht Nr. 10-04 (2010).
[12] O. Chubar, P. Elleaume, and J. Chavanne, Journal of Synchrotron Radiation **5**, 481 (1998).

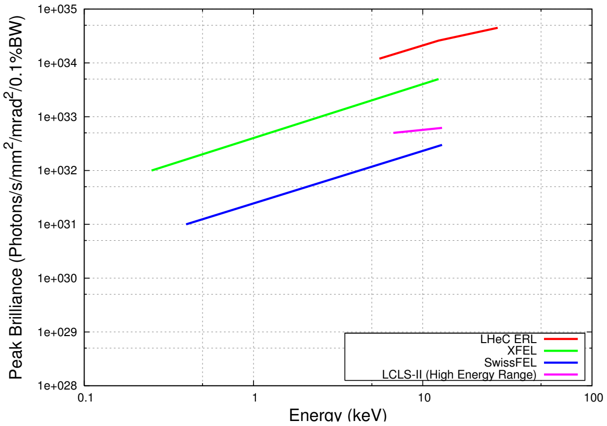

FIG. 8: Comparison of FEL peak brilliance for the LHeC-FEL with several existing or planned hard X-ray FEL sources.

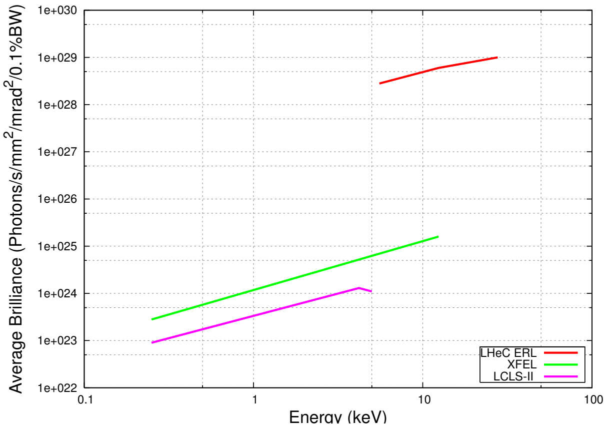

FIG. 9: Comparison of FEL average brilliance for the LHeC-FEL with existing and planned world-leading hard X-ray FEL sources.

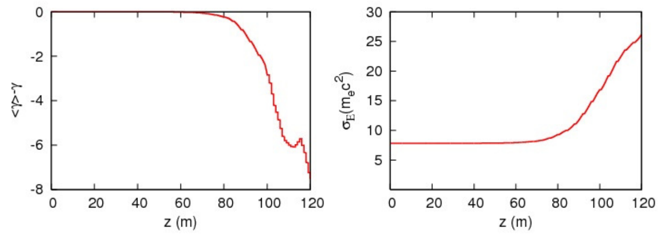

FIG. 10: Left: Evolution of the electron energy loss in units of gamma along the undulator region. Right: Evolution of the electron beam energy spread in units of the electron rest mass energy along the undulator region.

[13] S. Reiche et al., *Genesis User's Manual* (2004), available at `http://genesis.web.psi.ch/`.

[14] E.L. Saldin and E.A. Schneidmiller and M.V. Yurkov, *The Physics of Free Electron Lasers* (Springer, Berlin-Heidelberg, 2000).

[15] P. Schmüser, M. Dohlus and J. Rossbach, *Ultraviolet and Soft X-Ray Free-Electron Lasers* (Springer-Verlag Berlin-Heidelberg, 2008).

[16] J. Galayda (2015), BESAC Presentation.

[17] Makina Yabashi and Hitoshi Tanaka, NATURE PHOTONICS **11**, 12 (2017).

[18] J. C. Heminger et al. (2009).